

# Grid-scale Storage and Resource Adequacy Failures in Western U.S. Renewable Power System

by

Zihan Ye

A thesis submitted  
of the requirements for the degree of  
Master of Science  
(Environment and Sustainability)  
in The University of Michigan 2023

Committee:

Michael Craig

Parth Vaishnav

## Contents

Abstract.....	3
Objectives .....	3
Methods .....	4
Area of study.....	4
CEM.....	5
RE levels scenarios .....	5
Demand data .....	5
Capacity factors .....	5
RAM .....	6
Monte-Carlo iteration.....	6
Forced outage rates .....	7
Storage modification.....	7
SOM.....	7
Results.....	8
RA failure events distribution for the 2019 weather year .....	8
With increasing RE levels.....	8
With larger scale storage.....	9
Meteorological drivers for the 2019 weather year .....	10
Discussion .....	12
References.....	13

## Abstract

Despite extensive studies exploring the reliability aspects of Energy Storage Systems (ESS) within renewable energy systems, there remains an absence of investigation or establishment of a connection between Resource Adequacy (RA) failures and meteorology specifically for power systems incorporating grid-scale storage. This study aims to examine RA failures across varied levels of renewable energy penetration and grid-scale storage integration in the western U.S. and compare their meteorological drivers between power systems with and without storage integration. The power system is constructed using a capacity expansion model (CEM) that simulates the WECC power interconnection. The resource adequacy model (RAM) assesses resource sufficiency by identifying periods where supply and demand might potentially be imbalanced throughout a given year due to weather variations. The outputs from RAM are collected and categorized into weather patterns (WP) using a Self-Organizing Map (SOM) to identify meteorological drivers. The results highlight two main effects of grid-storage implementation in sustainable energy systems: a shift towards narrower and later time windows for RA failures, and a more varied set of Weather Pattern (WP) drivers for these failures. With storage implementation, the timeframe for risky hours compresses to roughly a 4-hour window, usually occurring after 6 PM. Concurrently, there's a considerable reduction in the total count of risky hours, decreasing notably to just a few instances. The meteorological drivers for fleets implemented with storage differ annually with varying levels of RE, implying unique WP impacts for each fleet. Notably, impactful WPs predominantly fall within the range of WP8, 9, and 10, mirroring the meteorological drivers observed in fleets without storage installation. The study offers an extension opportunity based on the timeframe differences in RA profiles resulting from grid-scale storage. Simulating RA failures enables an examination of grid-scale storage's impact on human well-being, particularly concerning household temperature control and access to cooling during heat waves.

## Objectives

The foreseeable increase in renewable energy (RE) integration within the grid over the coming decades raises concerns about the reliability of power systems operating at high RE levels, prompting considerations in power system planning. Resource Adequacy (RA) failures, often leading to large-scale outages, can arise due to intricate meteorology-influenced interactions between demand and supply, particularly as reliance on wind and solar energy intensifies. In this context, Energy Storage Systems (ESS) are gaining importance as they substantially mitigate renewable curtailment, enhance power system reliability, and ensure RA. (Blanco & Faaij, 2018).

Meteorological drivers become increasingly important in the context of the energy transition. Not only will surface air temperature affect the demand and supply for the grid, but solar radiation and wind speed will also significantly impact grid dispatch in a highly renewable power system. Moreover, the fragility of energy infrastructure under extreme weather and abnormal regional climate conditions poses another potential risk that can be enveloped by meteorological drivers analysis (Sundar et al., n.d.).

Many papers have demonstrated the outstanding performance in mitigating the RA failures of the integration of ESS with a renewable grid. It has been verified that the best reliability for a wind-integrated grid is reached when an auxiliary storage unit is equipped (Hussein & Al Muhaini, 2016). Liu, et al. chose the universal generating function to investigate a grid-scale battery ESS and proposed a configuration of the battery modules that can improve the reliability of the power system further (Liu et al., 2017). Parvini, Zohreh, et al. used a

modified PJM method to demonstrate that improvement of energy level as well as the charging strategy of ESS can effectively reduce the load and supply mismatch for the grid and increase its reliability (Parvini et al., 2018).

The following papers show some research findings on ESS's contribution to the energy system reliability. Bagen & Billinton investigated a small isolated power system with the same amount of conventional and renewable capacities and found its LOEE reduced by over 80% as a result of ESS integration (Bagen & Billinton, 2005). Hu, Po, et al. demonstrated over 20% decrease of LOEE thanks to the ESS for an energy system with the restriction of 5% wind power capacity (Hu et al., 2009). Gao, Z. Y., et al. showed a over 95% LOEE drop when storage capacity is increased from 0 MWh to 40 MWh in a system with wind energy (Gao et al., 2010). Wang, P., et al. displayed a 86% reduction of monthly LOEE when a 100-MWh battery ESS is added into an energy system with a 15% wind penetration (Wang et al., 2012). Anderson, K.'s studies revealed that for a microgrid system, integrating renewable energy and battery ESS with conventional generators provides cost savings and 1.8 to 4 days added resiliency time at 90% probability of outage survivability (Anderson et al., 2018). A more recent research echoed the prior results about the LOLE and LOEE drop attributable to ESS. Dratsas et al. revealed a 86.3% decrease of LOEE and a 82.8% decrease of LOLE initiated by BESS in a medium-sized island energy system (Dratsas et al., 2021)

Despite thorough studies on the reliability contributions of ESS for renewable energy systems, none of the aforementioned papers have connected RA failures with meteorology. Neither has a study modeled nor analyzed the impacts of climate change or regional weather on the reliability of an energy system incorporating ESS. Srihari's work presented a novel and comprehensive approach addressing the relationships between RA failures and meteorological drivers in power systems with high RE penetrations (Sundar et al., n.d.). However, this work failed to include storage considerations in its high-RE energy system analysis.

To fill the research gap, the thesis aims to achieve three main objectives. Firstly, the author aims to investigate power system RA failures and their characteristics at different levels of renewable energy penetration and grid-scale storage integration within the western U.S. power system. Secondly, the study will analyze the meteorological drivers contributing to these power system resource failures. Lastly, the research will explore and compare the similarities and differences in meteorological drivers between power systems with and without storage integration.

## Methods

### Area of study

The study area is the Western Interconnection overseen by Western Electricity Coordinating Council (WECC). It is chosen because of its relatively high renewable energy penetration level, where solar and wind generation in 2020 reached roughly 13% of the demand (State of the Interconnection, 2021). There are 27 main balancing authorities considered within the WECC area. The balancing authorities have been grouped into 5 subregions: CAMX, desert southwest, NWPP central, NWPP-NE, and NWPP-NW. The mapping of balancing authorities to the subregions as showed in Figure 1 is used in demanding aggregation for CEM modeling.

Sub-region	Balancing Authorities aggregated to find demand
CAMX	CISO, BANC, TIDC, LDWP
Desert Southwest	IID, AZPS, SRP, EPE, PNM, TEPC, WALC
NWPP Central	NEVP, PACE, IPCO, PSCO
NWPP NE	WACM, NWMT, WAUW, PACE
NWPP NW	PSEI, DOPD, CHPD, AVA, TPWR, GCPD, BPAT, PGE, PACW, SCL

Figure 1 Sub-region Table (Sundar et al., n.d.)

## CEM

Capacity expansion model is an optimization-based tool for fleets construction under customized constrains including capacity investment, units operations, inter-regional electricity transfer, planning reserve margin, solar to wind capacity ratio etc. with the goal of the system costs minimization. The plain fleets constructed by CEM output a capacity structure across WECC with regional information about power plants and a fixed RE generation level. The economic related parameters follow the moderate scenario for NREL annual technology baseline (ATB) year 2021(Sundar et al., n.d.). Fleets are unique for every weather and each RE level. The weather years range for this study is 2016-2019. Three of the most important constraints, RE levels, demand meeting, wind and solar capacity factors are elaborated in this section. Follow Sundar's work for more details (Sundar et al., n.d.).

### RE levels scenarios

There are three scenarios for renewable energy penetration requirements. The RE penetration levels are set as 13%, 20%, 40% for the power system generation in this study. The values were chosen based on the reality level (the current RE penetration in the WECC grid), the short-term (5-10 years) and long-term (10-20 years) projections (State of the Interconnection, 2020) correspondingly.

### Demand data

The hourly demand data are collected from the local balancing authorities (BA) with regional aggregation process as elaborated in Figure 1. All of the electricity demand data comes from the governmental publication, the EIA 930 forms (*Survey Forms - U.S. Energy Information Administration (EIA)*, n.d.). BAs' hourly demand is reported in Coordinated Universal Time (UTC). For meteorological analysis consistency, the time has been shifted to Pacific Standard Time (PST) in the US for this study.

### Capacity factors

To simulate the power generation for wind and solar, the hourly generation is constrained by the local capacity factors for the power plants. The meteorological resolutions for capacity factors were obtained from the ERA5 reanalysis dataset(Olauson, 2018). Key calculation process are summarized below.

$CAP_{c_{re}}$  is the current installed capacity of the generators at a grid location and  $k$  is the scale variable for CEM expansion control. The unit's generation is limited by its capacity and the capacity factor  $CF_{c_{re}}^t$  at each hour  $t$  and each grid point resolution  $c_{re}$ .

$$cap_{c_{re}} = k \times CAP_{c_{re}}, \forall c_{re} \in \mathbb{C}_{re} \quad \text{Equation 1}$$

$$gen_{c_{re}}^t \leq cap_{c_{re}} \times CF_{c_{re}}^t, \forall t \in T \quad \text{Equation 2}$$

For solar capacity factors calculations,  $RSDS$  surface downwelling shortwave flux [ $\text{Wm}^{-2}$ ],  $T_{cell}$  PV cell temperature,  $TAS$  surface air temperature (2m temperature), and,  $SWS$  surface wind speed (calculated from 10m u- and v- components of wind) were inserted in a linear

function  $f$  at Equation 4 (Tamizhmani et al., 2003).

$$\gamma = -0.005^{\circ}\text{C}^{-1}, T_{STC} = 25^{\circ}\text{C}$$

$$CF_{pv}^t = (1 + \gamma(T_{cell} - T_{STC})) \frac{RSDS^t}{RSDS_{STC}}, \quad \text{Equation 3}$$

$$T_{cell} = f(TAS, RSDS, SWS) \quad \text{Equation 4}$$

For wind capacity factors, we used the formulation Equation 5 for the 1.5 MW IEC class III turbine with power curves from the System Advisor Model (Blair et al., 2018) :

$$CF_{wind}^t = p(wind_{100m}^t) \quad \text{Equation 5}$$

$$p = f(TAS, HUSS, PS, \rho_d) \quad \text{Equation 6}$$

$p$  is the correction function for  $wind_{100m}^t$  100m wind speed at hour  $t$ . Equation 6 contains weather data including  $TAS$  surface air temperature,  $HUSS$  the surface specific humidity,  $PS$  surface pressure, and  $\rho_d$  dry air density (Bolton, 1980).

## RAM

The resource adequacy model quantifies the sufficiency of resources by identifying periods of potential imbalance between supply and demand throughout a weather year. At the core of this model lies a Monte Carlo-based non-sequential state sampling method. This method iterates 1,000 times, simulating potential outages by introducing randomness to samples taken from each power generator in the fleet, hourly, across the entire weather year. The RAM's mechanism involves assigning outage rates to individual power generation units by translating local ambient air temperatures using specific outage rate functions. These functions are unique to each power technology, and the outages simulated by RAM are contingent upon the prevailing local meteorological conditions. Storage units, regardless of weather conditions, are assumed to have an outage rate of 0. MC sampling process generates a dispatch curve spanning a year, which is then overlaid with the observed demand curve for that year. Hours where the demand surpasses the dispatch are classified as Loss of Load Hours (LOLH). The aggregation of probabilities across all 10,000 simulations yields the Loss of Load Possibility (LOLP) for that specific hour. If the LOLP exceeds a predetermined threshold, such as the 0.005 set in this particular study, that hour is categorized as a risky hour. These risky hours collectively form RA failure profiles for a given fleet. The Annual LOLP, obtained by summing LOLPs across the year, has been adjusted to 2.4 by either adding or removing Natural Gas Combined Cycle (NGCC) units from the fleet. This targeted value aligns with the real-world 1-in-10 reliability standard commonly adopted by utility companies.

## Monte-Carlo iteration

The quantity of Monte Carlo iterations significantly affects the RAM results. A larger MC iteration size leads to a reduction in the annual LOLP values variation, narrowing down the range of results (Sundar et al., n.d.). However, employing a larger iteration size demands increased computational power and time. To strike a balance between precision and computational efficiency, an iteration size of 10,000 has been selected. This choice aims to achieve a reasonable level of accuracy within manageable computational timeframes.

### Forced outage rates

NGCC, hydro power, solar and wind are associated with 3 distinct outage rate functions, intricately linked to and influenced by the ambient temperature. The functions are simplified to discrete mapping groups showed as Figure 2 (Sundar et al., n.d.).

Closest temperature value [ $^{\circ}C$ ]	-15	-10	-5	0	5	10	15	20	25	30	35
NGCC	14.9	8.1	4.8	3.3	2.7	2.5	2.8	3.5	3.5	4.1	7.2
Hydro	7	4.3	3.2	2.7	2.6	2.6	2.7	2.7	2.5	2.9	8.2
Solar, wind	5	5	5	5	5	5	5	5	5	5	5

Figure 2 Temperature dependent forced outage rates of different generators

### Storage modification

Due to economic constraints, the plain fleets generated by has no storage capacities in the fleet at the first place. The fleets modification task is to manually install while maintaining the system's reliability level as the original fleets for consistency. The storage modification consists of storage installation and NGCC retraction.

To install grid-scale storage, there are two assumed scenarios. The first one is based on the current battery storage capacity in the grid of CAISO. With 5,000 MW dispatch availability, around 6% of the total capacity of the grid is battery storage (*NEWS RELEASE*, 2023). The same percentage is used in the fleets simulation modification. The installed capacity is assumed to be 6% of the total capacity of the original fleets constructed in CEM. For the second scenario, the battery capacity is assumed to be 24% of the original capacity. The four-fold increase reflects the California grid transit plan by 2035 (Newsom, 2023).

Upon the installation of additional storage capacity, the energy system experiences an increase in reliability levels and a subsequent reduction in the annual LOLP. To restore the system to its original reliability level, a specific quantity of NGCC capacity is withdrawn, a value determined through an iterative process within the RAM. The RAM operates in a loop mode. The NGCC retraction capacity is decreased if the annual LOLP of the system is lower than 2.4 and increased if the annual LOLP become higher than 2.4. The process is repeated till the annual LOLP reaches 2.4. As a result of the Monte Carlo logic used, the withdrawn NGCC capacities vary with different settings within each Monte Carlo cycle, resulting in differing capacities for every calculation round. Different from the general RAM analysis, at the storage modification stage, the MC cycle is set as 500 because of computational power and time limitation. Additionally, the installed storages are assumed to possess a forced outage rate of 0, a power-to-energy ratio of 4 hours, and no segmentations, operating as a single, undivided unit following a reliability dispatch strategy.

### SOM

The meteorological drivers are identified by Self-organizing Map, a neural-network-based clustering technique. The weather regimes coincide with risky hours output from RAM are collected and categorized into clusters that are typical enough to be weather patterns (WP) in the WECC region. The clustering process is realized by SOM. Weather regimes are built based on seasonal anomalies of the daily average 500 hPa geopotential height (Z500) for the period spanning May through September from 1981-2020. 3x4 map is chosen for its clarity and low quantization error and topographic error. The 12 WPs shown in Figure 3 are produced with a gaussian neighborhood function, sigma value of 2, learning rate of 0.1, and 5,000 training iterations (Sundar et al., n.d.).

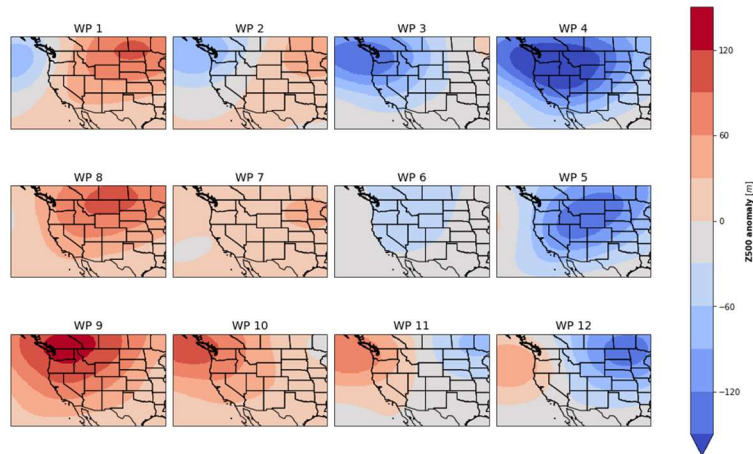


Figure 3 SOM Weather Patterns

## Results

The results are divided into two parts, RA profile analysis and meteorological drivers' comparison.

### RA failure events distribution for the 2019 weather year

#### With increasing RE levels

Figure 4 displays the RAM results of modified fleets in year 2019 with 6% grid-scale storage in the fleets with increasing renewable penetration. RA failures with different LOLP are scattered in chronological order along both x-axis and y-axis. Every star on the graph represents a risky hour with a bigger plot area reflecting a higher LOLP. Additionally, a red circle is employed to denote risky hours that occur in fleets with storage but are absent in the fleets without storage. Observing the three LOLHs distributions under increasing RE level, some conclusions can be drawn.

Across three RE levels, all risk hours occur in summer months, spanning from June to September. In fleets lacking storage, a majority of these risky hours tend to occur within the timeframe from 12 to 6 PM PST. Conversely, when compared to RA profiles excluding storage, fleets integrated with storage exhibit a more condensed distribution of risky hours. With storage implementation, the time range of risky hours becomes compressed to approximately a 4-hour window, typically emerging after 6 PM. Simultaneously, there is a significant reduction in the total count of risky hours, dropping notably to a handful of instances.

The concentration trend of LOLHs influenced by grid-scale storage is evident across all RE levels, albeit with slight variations. In the scenario with a 13% RE level, the introduction of 6% storage implementation leads to a delay in LOLHs, occurring within the timeframe of 6 to 10 PM. In the 20% RE level scenario, the LOLHs are shifted from predominantly occurring in the afternoons to a later timeframe of 8 to 12 PM. Similarly, under the 40% RE level scenario, the LOLHs are observed between 8 PM and extend into the following day until 1 AM. This trend illustrates how the presence of grid-scale storage affects the timing and concentration of RA failures across different levels of renewable energy integration.

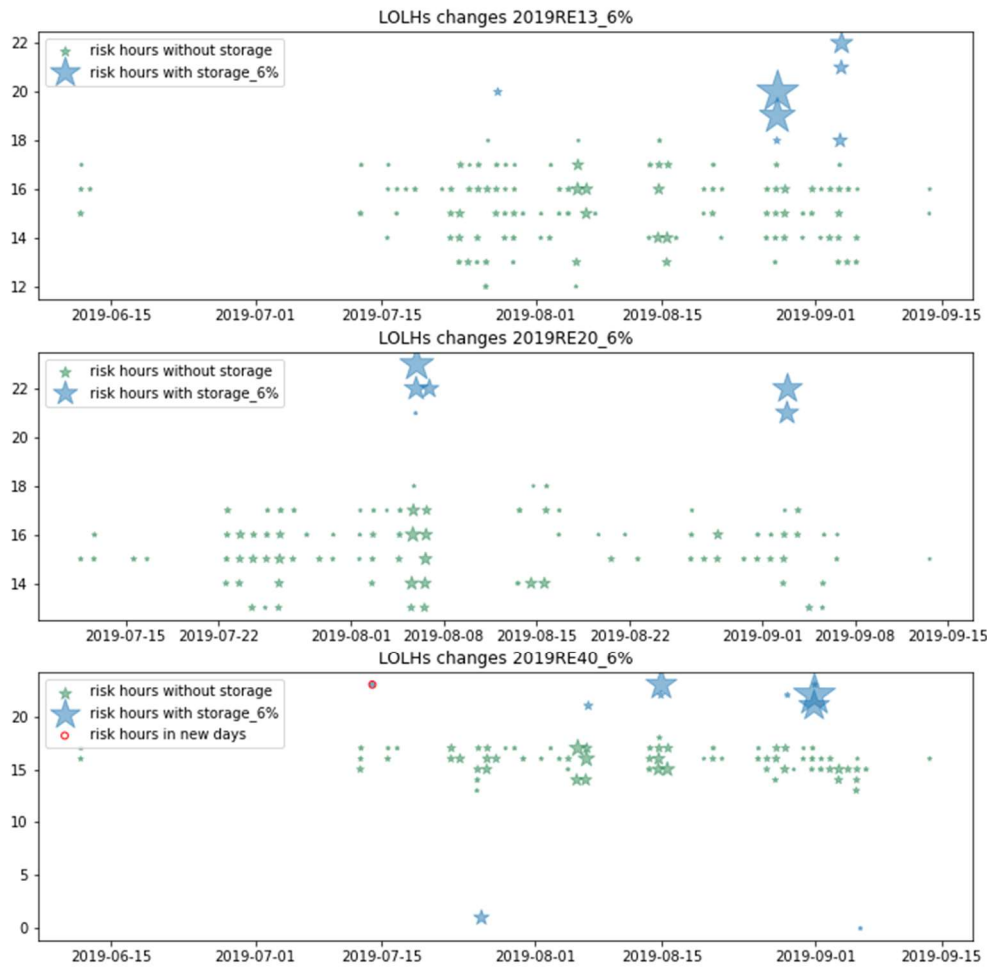


Figure 4 LOLHs distribution for the 2019 weather year scenario 1

### With larger scale storage

Figure 5 illuminates the discernible impact of a 20% grid-scale storage on the system dynamics. As observed similarly in the 6% storage scenario, the introduction of 20% storage concentration results in a compression of Loss of Load Hours (LOLHs) into a narrower and later timeframe. Moreover, due to the integration of storage, the occurrences of these critical events are drastically reduced to just a few instances.

However, with a larger scale of storage deployment, there is a more pronounced shift in LOLHs. In the 13% RE level scenario, instead of 6 to 10 PM, the introduction of 20% storage implementation results in LOLHs emerging between 8PM to midnight. In the 20% RE level scenario, the LOLHs are pushed to 9 PM till the following day. The 40% RE level scenario, the LOLHs are observed between 1 to 4 AM. Furthermore, in the 40% RE level scenario, the LOLHs are observed between 1 to 4 AM. This delay effect on the timing of Risked Hours caused by storage becomes more conspicuous with the integration of a larger capacity of storage.

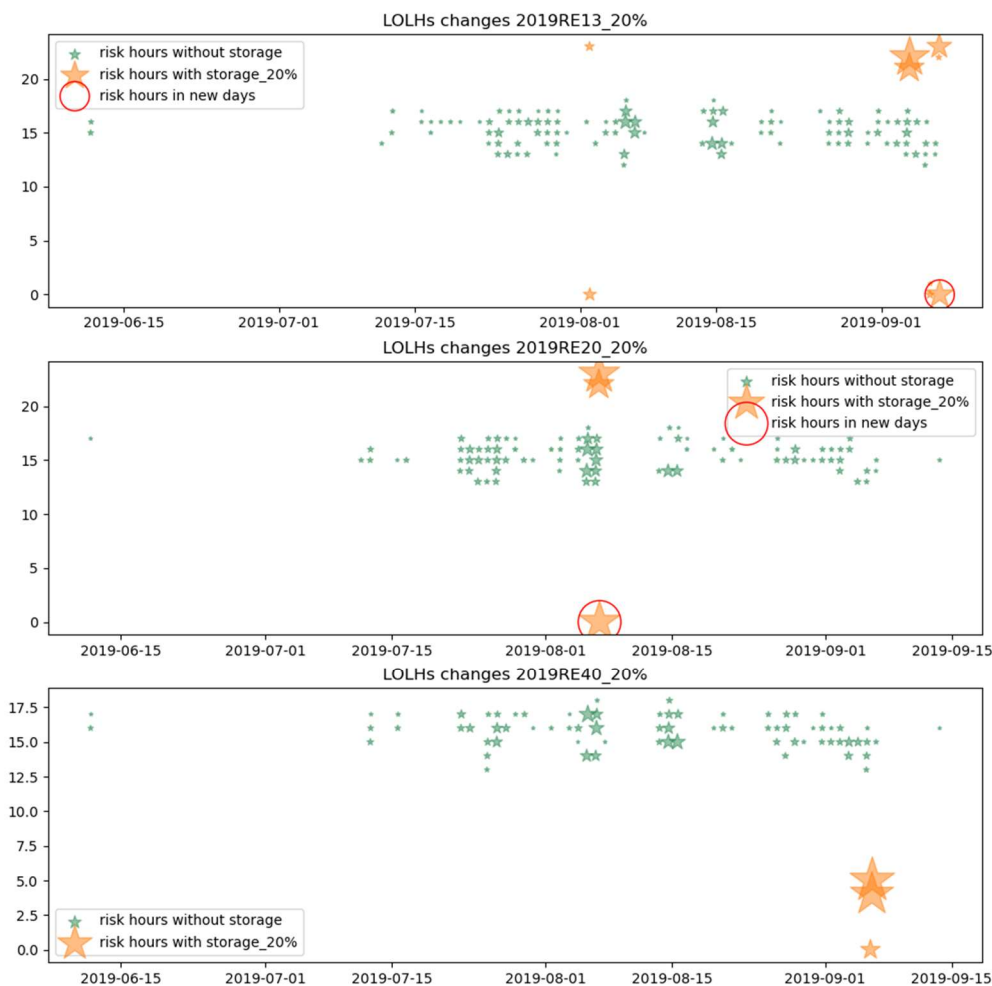


Figure 5 LOLHs distribution for the 2019 weather year scenario 2

### Meteorological drivers for the 2019 weather year

To link the RA profiles with the meteorological drivers, the specific days corresponding to the occurrence of risk hours are collected. Each of these risky days is associated with its own daily average Z500 weather regimes. By mapping these regimes to the weather patterns depicted in Figure 3, the meteorological profile for the RA failure for that date is established. A collection of the mapping results from 2019 fleets with 6% storage are shown in

Figure 6. For example, a LOLH occurs on July 25th 2019 according to the RAM results. Then the Z500 anomaly specific to this date is collected. Upon obtaining this anomaly data, it is then matched with the WPs output by the SOM. SOM indicates the WP for date July 25th is WP10, characterized by high-pressure anomalies situated in the northwest of the WECC region. Consequently, this LOLH event and its LOLP on July 25th contribute to or are associated with WP10 for further analysis regarding meteorological drivers. Among the WP collection in Figure 6, high-pressure anomalies predominantly characterize the risky days.

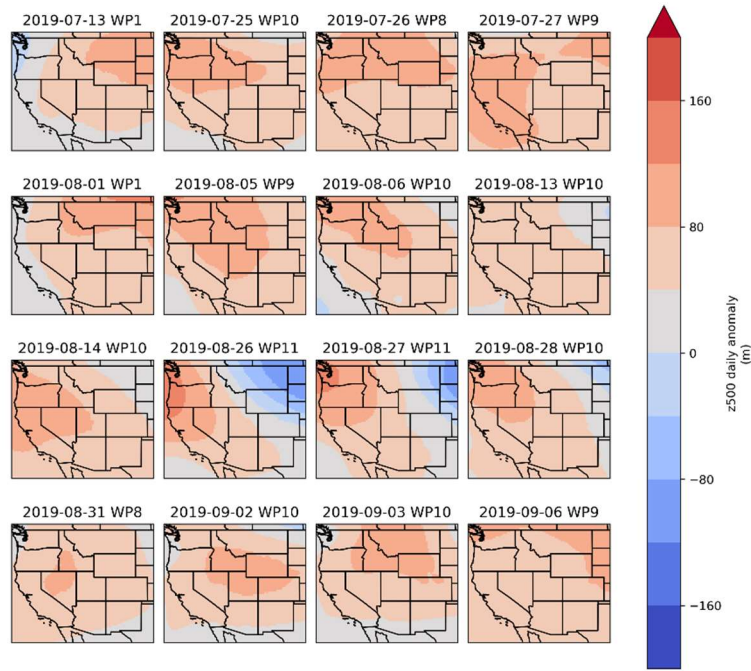


Figure 6 WP mapping for RA failure days for fleets with 6% storage for year 2019

By aggregating all the WPs corresponding to risk days alongside their accumulated LOLPs, predominant WPs can be found. A higher associated LOLP indicates a more significant impact of the respective WP. The numerical statistics comparison between fleets with and without storage are summarized in the following figure. The left y-axis and blue dots represent LOLPs for scenarios with storage, while the orange side illustrates the baseline without storage. Each WP comprises three data points, signifying situations across three RE levels.

The WP features for fleets without storage align with Sundar et al.'s results. There are three main drivers for RA failures, WP 7, 8, 9 with relatively flat trends when increasing RE penetration (Sundar et al., n.d.). Conversely, the systems integrated with grid-scale storage demonstrate distinct characteristics for each level of RE penetration. Figure 7 displays that in 2019, fleets integrated with 6% storage have main contributors to RA failures as WP8, 9, 10, and 11, with varying dominance in different RE levels. Specifically, at a 13% RE level, the most substantial meteorological driver is WP11; in the 20% RE system, WP10 stands out among other WPs; and for the 40% RE fleet, WP8 appears to have the most impact. Figure 8 illustrates the 20% storage scenario, where WP 8 and 10 account for most RA failures. WP8 predominantly affects the systems with 13% and 40% RE level and WP10 impacts the 20% RE case. Besides, when the system is integrated with grid-scale storage, the variation of WP dominance is sensitive to weather years according to the results from year 2016-2018. In other words, the meteorological drivers for fleets with diverse RE and storage levels differ across different years, indicating distinct WP impacts for each fleet. Nevertheless, the WPs that have significant impacts are within the range of WP8, 9, 10.

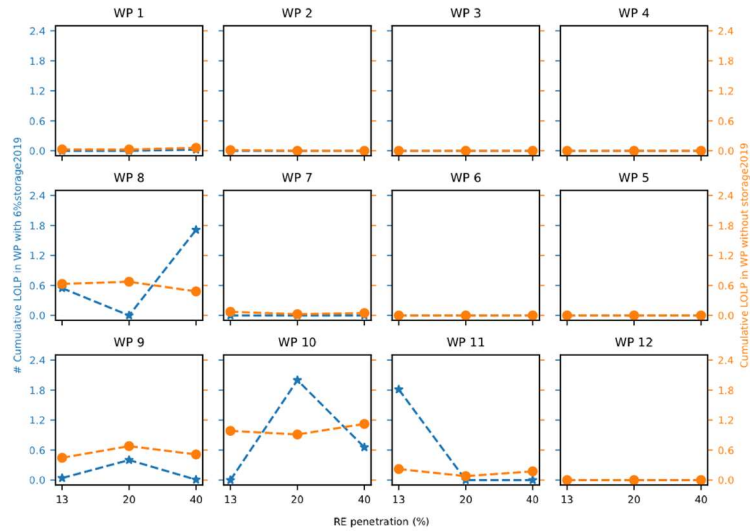


Figure 7 WPs comparisons between fleets with 6% storage and without storage for year 2019

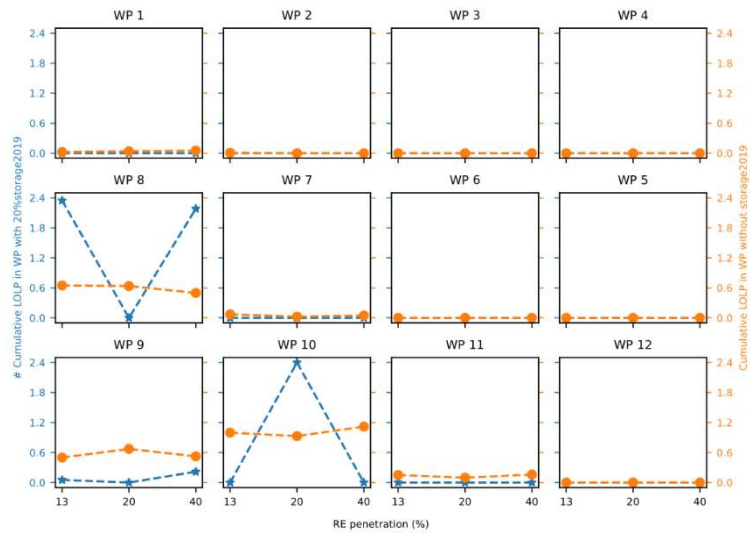


Figure 8 WPs comparisons between fleets with 20% storage and without storage for year 2019

## Discussion

The results indicate two primary effects resulting from grid-storage implementation in sustainable energy systems: firstly, a shift towards later and narrower time windows for RA failures; and secondly, a more diverse set of WP drivers for RA failures. The occurrences of LOLHs have been observed to dramatically decrease and transition from afternoons to late nights and even early mornings in systems featuring high RE levels and storage capacities. This phenomenon highlights the significance of grid-scale storage within the renewable power system. It showcases the grid-scale storage's role in concentrating risks emanating from distributed renewable power generators and underscores its capability in creating a lag effect on the mismatch between demand and supply. Meanwhile, meteorological drivers exhibit sensitivity to varying RE levels, storage capacities, and weather years. However, the most dominant WPs are within the range of WP8, 9, 10, that correspond to high pressure anomalies. The findings above are general across weather year 2016 to 2019.

The combination of high-pressure anomalies and RA failures raises concerns regarding

potentially severe outages that could jeopardize human well-being. Individually experiences temperature (IET) increases have been linked to higher mortality rates, particularly in cities with widespread air conditioning use (Stone et al., 2023). Research indicates that a 2-5 days lost of cooling in a Phoenix building can induce a 6.4 °C IET increase and a staggering 700% rise in heat mortality. The study offers an opportunity for extensions of our research. With the integration of grid-scale storage into the grid, the RA failures driven by high-pressure anomalies exhibit distinct timeframes compared to RA profiles for fleets lacking storage. By simulating the timeframe differences caused by outage events, it becomes possible to investigate the impact of grid-scale storage on human well-being, specifically in terms of household temperature control and access to cooling during heat waves.

## References

- Anderson, K., Laws, N. D., Marr, S., Lisell, L., Jimenez, T., Case, T., Li, X., Lohmann, D., & Cutler, D. (2018). Quantifying and monetizing renewable energy resiliency. *Sustainability (Switzerland)*, *10*(4). <https://doi.org/10.3390/su10040933>
- Bagen, & Billinton, R. (2005). Incorporating well-being considerations in generating systems using energy storage. *IEEE Transactions on Energy Conversion*, *20*(1), 225–230. <https://doi.org/10.1109/TEC.2004.842376>
- Blair, N., Diorio, N., Freeman, J., Gilman, P., Janzou, S., Neises, T., & Wagner, M. (2018). *System Advisor Model (SAM) General Description (Version 2017.9.5)*. [www.nrel.gov/publications](http://www.nrel.gov/publications).
- Blanco, H., & Faaij, A. (2018). A review at the role of storage in energy systems with a focus on Power to Gas and long-term storage. *Renewable and Sustainable Energy Reviews*, *81*, 1049–1086. <https://doi.org/10.1016/J.RSER.2017.07.062>
- Bolton, D. (1980). The Computation of Equivalent Potential Temperature. *Monthly Weather Review*, *108*(7), 1046–1053. [https://doi.org/10.1175/1520-0493\(1980\)108](https://doi.org/10.1175/1520-0493(1980)108)
- Dratsas, P. A., Psarros, G. N., & Papathanassiou, S. A. (2021). Battery energy storage contribution to system adequacy. *Energies*, *14*(16). <https://doi.org/10.3390/en14165146>
- Gao, Z. Y., Wang, P., & Wang, J. (2010). Impacts of energy storage on reliability of power systems with WTGs. *2010 IEEE 11th International Conference on Probabilistic Methods Applied to Power Systems, PMAPS 2010*, 65–70. <https://doi.org/10.1109/PMAPS.2010.5528976>
- Hu, P., Karki, R., & Billinton, R. (2009). Reliability evaluation of generating systems containing wind power and energy storage. *IET Generation, Transmission and Distribution*, *3*(8), 783–791. <https://doi.org/10.1049/iet-gtd.2008.0639>
- Hussein, I., & Al Muhaini, M. (2016). Reliability assessment of integrated wind-storage systems using Monte Carlo simulation. *13th International Multi-Conference on Systems, Signals and Devices, SSD 2016*, 709–713. <https://doi.org/10.1109/SSD.2016.7473689>
- Liu, M., Li, W., Wang, C., Polis, M. P., Wang, L. Y., & Li, J. (2017). Reliability Evaluation of Large Scale Battery Energy Storage Systems. *IEEE Transactions on Smart Grid*, *8*(6), 2733–2743. <https://doi.org/10.1109/TSG.2016.2536688>
- NEWS RELEASE. (2023). [www.caiso.com](http://www.caiso.com)
- Newsom, G. (2023). *BUILDING THE ELECTRICITY GRID OF THE FUTURE:*

*CALIFORNIA'S CLEAN ENERGY TRANSITION PLAN.*

- Olauson, J. (2018). ERA5: The new champion of wind power modelling? *Renewable Energy*, 126, 322–331. <https://doi.org/10.1016/j.renene.2018.03.056>
- Parvini, Z., Abbaspour, A., Fotuhi-Firuzabad, M., & Moeini-Aghtaie, M. (2018). Operational Reliability Studies of Power Systems in the Presence of Energy Storage Systems. *IEEE Transactions on Power Systems*, 33(4), 3691–3700. <https://doi.org/10.1109/TPWRS.2017.2771521>
- State of the Interconnection.* (2023).
- Stone, B., Gronlund, C. J., Mallen, E., Hondula, D., O'Neill, M. S., Rajput, M., Grijalva, S., Lanza, K., Harlan, S., Larsen, L., Augenbroe, G., Krayenhoff, E. S., Broadbent, A., & Georgescu, M. (2023). How Blackouts during Heat Waves Amplify Mortality and Morbidity Risk. *Environmental Science and Technology*, 57(22), 8245–8255. <https://doi.org/10.1021/acs.est.2c09588>
- Sundar, S., Craig, M. T., Payne, A. E., Brayshaw, D. J., & Lehner, F. (n.d.). *Meteorological drivers of resource adequacy failures in current and high renewable Western U.S. power systems.* <https://doi.org/10.1038/s41467-023-41875-6>
- Survey Forms - U.S. Energy Information Administration (EIA).* (n.d.). Retrieved December 2, 2023, from <https://www.eia.gov/survey/#eia-930>
- Tamizhmani, G., Ji, L., Tang, Y., Petacci, L., & Osterwald, C. (2003). *Photovoltaic Module Thermal/Wind Performance: Long -Term Monitoring and Model Development For Energy Rating.*
- Wang, P., Gao, Z., & Bertling, L. (2012). Operational adequacy studies of power systems with wind farms and energy storages. *IEEE Transactions on Power Systems*, 27(4), 2377–2384. <https://doi.org/10.1109/TPWRS.2012.2201181>